1 **QTL mapping of natural variation reveals that the developmental regulator**

2 ***bruno* reduces tolerance to *P*-element transposition in the *Drosophila* female**

3 **germline**

4 Erin S. Kelleher[*†], Jaweria Jaweria[*], Uchechukwu Akoma[*‡], Lily Ortega[*] and Wenpei

5 Tang[*].

6

7

8

[*] Department of Biology and Biochemistry, University of Houston, Houston, TX
[†] To whom correspondence should be addressed: eskelleher@uh.edu
[‡] Department of Molecular Physiology and Biophysics, Baylor College of Medicine, Houston, TX, US 77030

ABSTRACT

Transposable elements (TEs) are obligate genetic parasites that propagate in host genomes by replicating in germline nuclei, thereby ensuring transmission to offspring. This selfish replication not only produces deleterious mutations---in extreme cases, TE mobilization induces genotoxic stress that prohibits the production of viable gametes. Host genomes could reduce these fitness effects in two ways: resistance and tolerance. Resistance to TE propagation is enacted by germline specific small-RNA-mediated silencing pathways, such as the piRNA pathway, and is studied extensively. However, it remains entirely unknown whether host genomes may also evolve tolerance, by desensitizing gametogenesis to the harmful effects of TEs. In part, the absence of research on tolerance reflects a lack of opportunity, as small-RNA-mediated silencing evolves rapidly after a new TE invades, thereby masking existing variation in tolerance.

We have exploited the recent the historical invasion of the *Drosophila melanogaster* genome by *P*-element DNA transposons in order to study tolerance of TE activity. In the absence of piRNA-mediated silencing, the genotoxic stress imposed by *P*-elements disrupts oogenesis, and in extreme cases leads to atrophied ovaries that completely lack germline cells. By performing QTL-mapping on a panel of recombinant inbred lines (RILs) that lack piRNA-mediated silencing of *P*-elements, we uncovered multiple QTL that are associated with differences in tolerance of oogenesis to *P*-element transposition. We localized the most significant QTL to a small 230 Kb euchromatic region, with the LOD peak occurring in the *bruno*

locus, which codes for a critical and well-studied developmental regulator of oogenesis. We further demonstrate that multiple *bruno* loss-of-function alleles are strong dominant suppressors of ovarian atrophy, allowing for the development of mature egg-chambers in the face of *P*-element activity. Genetic and cytological analyses suggest that *bruno* tolerance is explained by enhanced retention of germline stem cells in dysgenic ovaries, which are typically lost due to DNA damage. Our observations reveal segregating variation in TE tolerance for the first time, and implicate gametogenic regulators as a source of tolerant variants in natural populations.

INTRODUCTION

Transposable elements (TEs) are omnipresent and abundant constituents of eukaryotic genomes, comprising up to 80% of genomic DNA in some lineages (reviewed in [1]). The evolutionary footprint of TEs is extensive, including dramatic genome size expansions [2,3], acquisition of new regulatory networks [4,5], structural mutations [6], novel genes [7–9], and adaptive insertions [10–12]. However, the charismatic and occasionally beneficial impact of TEs over evolutionary time masks their fundamental identity as intragenomic parasites and mutagens. In addition to causing deleterious mutations [13,14], TEs can exert lethal, genotoxic effects on host cells by producing abundant double-stranded breaks (DSBs) during insertion and excision [15,16]. TEs are therefore intragenomic parasites.

Host developmental and evolutionary responses to parasites, pathogens, and herbivores are broadly delineated into two categories: resistance and tolerance (reviewed in [17,18]). Mechanisms of resistance prevent—or limit the spread of—infection or herbivory. By contrast, mechanisms of tolerance do not effect the propagation, but rather limit the fitness costs to the host. With respect to TEs, resistance by eukaryotic genomes is enacted by small RNA mediated silencing pathways [19], and Kruppel-associated box zinc-finger proteins (KRAB-ZFPs)[20], which regulate the transcription and subsequent transposition of endogenous TEs. However, it remains unknown whether genomes can also evolve tolerance of TEs, by altering how host cells are affected by TE activity. Tolerance therefore represents

a wholly unexplored arena of the evolutionary dynamics between TEs and their hosts. Germline tolerance of TEs is predicted to be of particular importance, due to the significance of this cell lineage in ensuring the vertical transmission of the parasite, and the reproductive fitness of the host.

The absence of research on tolerance is at least partially due the primacy of resistance: endogenous TEs are overwhelmingly repressed by host factors in both germline and somatic tissues [19,21,22]. However, the invasion of the host genome by a novel TE family, which happens recurrently over evolutionary time scales (reviewed in [23]), provides a window of opportunity through which tolerance could be viewed, both empirically and by natural selection. The absence of evolved resistance in the host against a new invader could reveal differential responses of germline cells to unrestricted transposition. A classic example of genome invasion by a novel TE is provided by *P*-elements, DNA transposons that have recently colonized two *Drosophila* species. *P*-elements first appeared in genomes of *D. melanogaster* around 1950 (reviewed in [24]), and later colonized it's sister species *D. simulans* around 2006 [25,26]. Particularly for *D. melanogaster*, a large number of naïve strains collected prior to *P*-element invasion are preserved in stock centers and laboratories, providing a record of ancestral genetic variation in tolerance [27,28]. Furthermore, 15 of these naïve strains were recently used to develop the *Drosophila* Synthetic Population Resource (DSPR), a panel of highly Recombinant Inbred Lines (RILs) that serve as a powerful toolkit for discovering the natural genetic variants influencing quantitative traits [29–31].

Here, we harness the mapping power of the DSPR to screen for phenotypic and genetic variation in the tolerance of the *D. melanogaster* female germline to unrestricted *P*-element activity. We developed a novel screen for phenotypic variation in host tolerance by taking advantage of the classic genetic phenomenon of hybrid dysgenesis, in which TE families that are inherited exclusively paternally can induce a sterility syndrome in offspring, due to an absence of complementary maternally-transmitted regulatory small RNAs (piRNAs, reviewed in [24,32,33]). The dysgenesis syndrome induced by *P*-elements in the female germline is particularly severe, and can be associated with a complete loss of germline cells [15,34,35]. *P*-element hybrid dysgenesis is directly related to genotoxic stress, as apoptosis is observed in early oogenesis in dysgenic females [15], and the DNA damage response factors *checkpoint kinase 2* and *p53* act as genetic modifiers of germline loss [35]. Variation in the sensitivity of the DNA damage response to double-stranded breaks therefore represents one potential cellular mechanism for tolerance.

By phenotyping the germline development of >32,000 dysgenic female offspring of RIL mothers, we uncovered substantial heritable variation in female germline tolerance of *P*-element activity. We furthermore mapped this variation to a small 230 Kb quantitative trait locus (QTL) on the second chromosome, containing only 18 genes. Only one locus, *bruno*, is a strong candidate for the source of causative variation. Surprisingly, *bruno* encodes a well-studied developmental regulator of oogenesis, with no known function in TE repression or DNA damage response [36–39]. We further demonstrate that *bruno* loss-of function alleles act as

dominant suppressors of germline loss, and relate these effects to the retention of germline stem cells (GSCs) in dysgenic females. Our findings represent the first demonstration of natural variation in TE tolerance in any organism. They further implicate regulators of gametogenesis such as *bruno*, as a source of tolerant variants that could be beneficial when new TEs invade the host.

RESULTS

Maternal genotype, but not zygotic age, is a strong predictor of dysgenic F1 atrophy.

We first sought to uncover phenotypic variation in germline tolerance of *P*-element activity among a panel of highly recombinant inbred lines (RILs) derived from eight founder genomes [29]. To quantify tolerance, we performed dysgenic crosses between RIL females and males from the *P*-element containing strain Harwich (Figure 1A). Harwich is a strong paternal inducer of hybrid dysgenesis, producing F1 females with 100% atrophied ovaries in crosses with naïve females at the restrictive temperature of 29°C [28]. We therefore performed our crosses at 25°C, a partially permissive temperature at which intermediate levels of ovarian atrophy are observed [40,41]. Because *P*-element dysgenic females may recover their fertility as they age, through zygotic production of *P*-element derived piRNAs [42], we assayed both 3-day old and 21-day old F1 female offspring from each RIL. In total, we documented the incidence of atrophied ovaries among 17,150 3-day-old

and 15,039 21-day-old F1 female offspring, and estimated the proportion of F1 atrophy within broods of $\geq$ 20 3-day old and 21-day old offspring from 592 and 492 RILs, respectively (Figure 1B, 1C).

We observed continuous variation in the proportion of F1 atrophy among both 3-day old and 21-day old offspring of different RIL genotypes (Figure 1B, 1C). After accounting for the effects of experimenter and experimental block, the incidence of ovarian atrophy is strongly correlated among 427 RILs for which we sampled broods of both 3-day old and 21-day old F1 females (Pearson's $R = 0.56$, $p > 10^{-15}$, Figure 1D). Because broods of different age classes were sampled from separate crosses and experimental blocks, this correlation strongly implies that phenotypic differences are explained by the maternal genotype. Indeed, based on the F1 atrophy proportions measured in broods of different ages, we estimate that the broad-sense heritability of F1 ovarian atrophy among the RIL offspring was 40.35% (see Materials and Methods). Furthermore, we saw greater reproducibility across a small sample of 14 RILs for which we phenotyped two independent 21-day broods (Pearson's $R = 0.97$, $p > 10^{-8}$), suggesting even higher heritability among offspring of the same age class.

Despite the previous observation of developmental recovery from hybrid dysgenesis [42], the relationship between age and the proportion of F1 atrophy is only marginally significant in our data (*Likelihood Ratio Test* = 3.60, $p = 0.058$). Furthermore, 21-day old dysgenic females exhibited only a 0.63% decrease in the proportion of F1 atrophy when compared to 3-day old females, indicating that the overall effect of age in our crosses was very modest. Finally, we did not observe a

group of RILs in which ovarian atrophy is much more common among 3-day-old as compared to 21-day-old F1 females (Figure 1D), as would be predicted if there were genetic variation for development recovery across the RIL panel. The absence of developmental recovery of in our experiments could reflect differences in developmental temperature between our two studies (22°C in [42] and 25°C here). Alternatively, the causative variant that allows for developmental recovery could be absent from the founder RILs.

QTL Mapping of Dysgenic F1 Atrophy.

To identify the genomic regions that harbor causative genetic variation in tolerance, we performed a QTL analysis using the published RIL genotypes [29]. In these data, the founder allele (A1-A8) carried by each RIL is inferred probabilistically for 10 Kb windows along the euchromatic regions of the major autosomes 2 and 3, and the X-chromosome [29]. The fourth chromosome is ignored because the absence of recombination makes it uninformative for QTL mapping (reviewed in [43]).

Consistent with the strongly correlated phenotypes of 3-day-old and 21-day-old offspring (Figure 1D), we identified a single major effect QTL associated with phenotypic variation at both developmental time points (Figure 2A). Additionally, the Δ2-LOD drop confidence intervals (Δ2-LOD CI) of the LOD peak from each analysis are both narrow (<300 Kb) and highly overlapping (Table 1). The peak explains 14.2% and 14.8% of variation in ovarian atrophy among 3-day-old and 21-

day-old F1 females, indicating it is a major determinant of heritable variation. Multiple minor peaks close to the centromere of 3L may represent another source of heritable variation in 3-day-old females.

To further narrow the location of genetic variation in tolerance, we took advantage of the striking concordance in QTL mapping for the 3-day old and 21-day old datasets, and performed a combined analysis including all 660 RILs whose F1 offspring were sampled at either developmental time point. F1 female age was included as a covariate (see methods). From this analysis we obtained a final Δ2-LOD CI for the major QTL peak, which corresponds to a 230 Kb genomic region containing 18 transcribed genes, 15 protein-coding and 3 non-coding (Figure 2B). Simulation testing of the statistical properties of the DSPR indicate that a causative variant explaining 10% of phenotypic variation lies within the Δ2-LOD drop CI 96% of time for sample sizes of 600 RILs [30]. Therefore, given our increased sample (660 RILs) and effect (~14%) sizes, the Δ2-LOD CI we infer for our major peak should be conservative. Interestingly, of the genes within the QTL peak, only *bruno* and *crooked* are highly expressed in the *D. melanogster* ovary [44]. While *bruno* is translational repressor whose major essential role is in oogenesis [37,45,46], *crooked* is a more broadly expressed component of septate junctions, which is essential for viability [47]. The LOD peak resides within the 138 Kb *bruno* locus which, in addition to its function, make it the strongest candidate for the source of causative variation.

Two classes of tolerance alleles.

We next sought to partition founder alleles at the QTL peak into phenotypic classes, in order to better understand the complexity of causative genetic variation. First we identified all sampled RILs whose genotype was probabilistically assigned ($p > 0.95$) to a single founder (A1-A8) at the LOD peak, and estimated the phenotypic effect associated with each founder allele (Figure 3). We then used stepwise regression (see Materials and Methods) to identify the minimum number of allelic classes required to explain phenotypic variation associated with the founder alleles. For both age classes, we found strong evidence for 2-allelic classes, one sensitive and one tolerant, were sufficient explain phenotypic variation in tolerance. This implies that the major QTL peak could correspond to a single segregating genetic variant. Furthermore, with the exception of founder A8, founder alleles were assigned to the same allelic class for both age cohorts, revealing allelic behavior is highly biologically reproducible.

In light of the simple biallelic behavior of our phenotype, we sought to identify polymorphisms within the founder strains whose genotypic differences matched their phenotypic classifications (*i.e.* "in-phase" polymorphisms [29,31], Figure 3C). We excluded A8 from these analyses due to the ambiguity of its allelic class. In total we identified 36 in-phase single nucleotide polymorphisms (SNPs), which potentially affect the function of only seven transcribed genes in the QTL interval ([48] Supplementary Table 3, Figure 2B, Figure 3C). We did not identify any in phase, segregating TE insertions, although a recent re-assembly of the founder A4 genome based on long single-molecule real-time sequencing reads suggests many

TE insertions remain un-annotated [49]. 22 of the in-phase SNPs are within the *bruno* locus or immediately upstream, while none are found in the gene-body or upstream of *crooked*. None of the 36 in-phase SNPs are non-synonymous, implying a regulatory difference between the tolerant and sensitive alleles.

bruno is a strong dominant suppressor of _P_-element induced ovarian atrophy.

We next examined whether *bruno* loss of function alleles affected the atrophy phenotype. For comparison, we also considered available alleles from three other ovary-expressed genes that are located within the Δ2-LOD CI of the 21-day old or 3-day old female analyses, but not in the combined analysis: *ced-12*, *Rab6* and *ThrRS*. We reasoned that since the causative variant is almost certainly not recessive, being found only in the maternal RIL genotype, mutant alleles might also exhibit non-recessive effects. We therefore used balanced heterozygous females as mothers in dysgenic crosses with Harwich males, and compared the incidence of F1 ovarian atrophy among their 3-7 day-old F1 females (*mutant/+ vs. balancer/+,* Figure 4). Strikingly, while *ced-12, Rab6* and *ThrRS* alleles had no effect on the incidence of ovarian atrophy, two different *bruno* alleles ($bruno^{RM}$ and $bruno^{QB}$) acted as dominant suppressors. In contrast to their balancer control siblings, who exhibited 64-75% ovarian atrophy, $bruno^{RM}/+$ and $bruno^{QB}/+$ offspring exhibited only 13% and 20% atrophy, respectively, a dramatic reduction in the atrophy phenotype (Figure 4). We further observed that an independently-derived *bruno* deficiency [50,51] suppresses ovarian atrophy to a similar degree (Figure 5), indicating these

effects cannot be attributed to a shared linked variant on the *bruno*^{RM} and *bruno*^{QB} chromosomes [45]. Importantly, these non-recessive, fertility enhancing effects of *bruno* loss-of-function alleles in dysgenic females also contrast their effects on the fertility of non-dysgenic females, where they act as recessive female steriles [45].

bruno's effects on ovarian atrophy are associated with germline stem cell retention.

bruno is a translational regulator with three known functions in *Drosophila melanogaster* oognesis. At the start of oogenesis in the ovarian substructure called the germaria, *bruno* is required to promote the differentiation of cystoblasts (CBs) the immediate daughters of germline stem cells (GSCs) [37,52]. In mid-oogenesis, Bruno protein blocks vitellogenesis if not properly sequestered by its mRNA target *oskar* [38,39]. Finally, in late oogenesis, Bruno repression of *oskar* translation is required to establish dorsovental (DV) patterning in the subsequent embryo [36] . This final role of *bruno* affects only the morphology of egg chambers, and but not their production, suggesting that it can not account for *bruno's* effects in dysgenic germlines. We therefore focused on *bruno's* earlier roles in GSC differentiation and vitellogenesis, which are distinguishable by their dependency on *oskar* mRNA. While *bruno's* functions in GSC differentiation are independent of *oskar* mRNA [36,37,53], *bruno* and *oskar*'s impact on vitellogenesis are interdependent, due to the requirement for *oskar* mRNA to sequester Bruno protein [39].

To determine if the effect of *bruno* alleles on hybrid dysgenesis are independent of *oskar* mRNA, we examined whether two *oskar* mRNA null alleles, osk^{0} and osk^{A87}, as well as an *oskar* deficiency, affected the incidence of ovarian atrophy when compared to a balancer control. We observed that osk^{0} and *Df(3R)osk* exhibited no effect on the atrophy phenotype, while osk^{A87} was associated with only a marginal increase in ovarian atrophy (p = 0.07). If *bruno* suppression of ovarian atrophy reflects reduced sequestration by *oskar* mRNA in the dysgenic female germline, atrophy should be enhanced by *oskar* mutants.

Comparison of single and double heterozygotes of *bruno* and *oskar,* also suggest that *bruno* suppression occurs independently of *oskar* mRNA. *Df(2L)bru/+;* osk^{A87}/+; double heterozygotes did not differ from their single *Df(2L)bru/+;balancer/+* heterozygous siblings with respect to ovarian atrophy, suggesting that *bruno* suppression is unrelated to *oskar* dosage. Although a second double-heterozygote *Df(2L)bru/+;Df(3R)osk*/+; was associated with significantly increased atrophy when compared to the single heterozygote (*Df(2L)bru/+; balancer/+*), we suspect this is a consequence of the double-deficiency, because *Df(3R)osk* alone had no effect (Figure 5). We also did not detect any Bruno mislocalization in the developing egg chambers of wild-type dysgenic females (Supplementary Figure 1), nor did we see any evidence of an arrest in mid-stage oogenesis in wild-type dysgenic ovaries, as occurs when Bruno is not sequestered by *oskar* mRNA [38,39]. Taken together, these experiments strongly suggest that *bruno's* effects on oogenesis under *P*-element dysgenesis are independent of *oskar*.

To evaluate whether *bruno* suppression of ovarian atrophy could be explained by its *oskar*-independent role in GSC differentiation [52,54], we directly examined and compared GSCs between *bruno*^{QB}*/+* and *CyO/+* dysgenic ovaries. While did not observe any direct evidence of delayed GSC differentiation in *bruno*^{QB}*/+* germaria, we did observe that ovarioles containing developing egg chambers overwhelmingly retained all oogenic stages, including GSCs (Figure 6B). In contrast, atrophied ovaries lacked any developing egg chambers including GSCs (Figure 6A). These observations are consistent with recent evidence that GSC retention is a key determinant of *P*-element induced ovarian atrophy [35]. They further suggest that reduced *bruno* signaling for differentiation may stabilize GSCs in their niche, allowing them to be retained despite the genotoxic effect of *P*-elements.

DISCUSSION:

While the evolution of TE resistance through small-RNA-mediated silencing is a topic of immense research interest, the existence and evolution of tolerance factors that may reduce the fitness costs of TEs on the host remain undocumented. By opportunistically employing a panel of genotyped recombinant inbred lines, which uniformly lack small-RNA-mediated silencing of the recently invaded *P*-element, we have here uncovered the first example of segregating variation in host-TE tolerance in any organism. The natural variation in tolerance that we uncovered is unlikely to be exceptional. A complementary QTL analysis of tolerance in DSPR

mapping population B has revealed a distinct peak of major effect in a different genomic location (Lama and Kelleher, *unpublished*). Furthermore, major QTL peak that we identified here in population A explains only about 35% of the heritable variation in tolerance. Therefore, other segregating variants in the population A RILs must also affect female germline response to *P*-element activity. Our inability to map these variants likely reflects the fact that they are rare, exhibit small effects, or both [30].

While differences in tolerance may be masked by resistance after small-RNA-mediated silencing evolves, our study reveals that in the absence of silencing, tolerance can be a major determinant of fitness. While the major peak we identified is modest in it's functional effects, explaining ~14% of variation in ovarian atrophy, variation in fertility of this scale would be dramatic in the eyes of natural selection. Segregating tolerance alleles, such as the one we have detected here, could therefore be subject to strong positive selection during genome invasion by a novel TE. Tolerance may therefore be an important feature of the host evolutionary response to invading TEs. Indeed, the correlation between *P*-element dosage and the severity of hybrid dysgenesis is poor at best, causing many to suggest that other genetic factors, such as tolerance alleles, may also be important determinants of the dysgenic phenotype [55–57]. Furthermore, the hybrid dysgenesis induced by recent collections of *D. melanogster* tends to be mild when compared to collections from the 1970's and 1980's, providing circumstantial evidence that tolerance factors may have increased in frequency over time [57]. Once the causative variant responsible

for the tolerance phenotype we uncovered here is identified, we will be poised to ask whether its increase in frequency has enhanced tolerance in extant populations.

Based on its high expression in the *Drosophila* female ovary [44], the presence of 22 SNPs that are in-phase with founder QTL alleles, and the dominant suppressive effect of classical loss-of-function alleles on dysgenic ovarian atrophy, *bruno* is a very strong candidate for the source of causative variation in *P*-element tolerance that we mapped on chromosome 2L. Identifying the causative variant(s) within the very large (138 Kb) *bruno* locus, and understanding how its altered function relates to hybrid dysgenesis presents an exciting challenge for future work. On the surface, it is not obvious how *bruno* function could be related to *P*-element activity, since *bruno* is neither a TE regulator nor a component of the DNA damage response that responds to TE-induced genotoxicity. However, the connection is plausibly explained by *bruno*'s function in promoting GSC differentiation [37,52]. We recently have discovered that the DNA damage response factor p53 is ectopically activated in the GSCs and CBs of dysgenic germlines, indicating that *P*-element induced genotoxic stress begins at the earliest stages of oogenesis [35]. GSCs are destabilized and lost in the presence of DNA damage [58], which explains why GSCs are frequently absent from dysgenic ovaries (Figure 6, [15,34,35]). Because GSC maintenance also requires the repression of differentiation factors including *bruno* [54,59–61], we propose that *bruno* loss-of-function alleles could stabilize damaged GSCs in their niche in dysgenic germaria. Indeed, loss-of-function mutations in two other GSC differentiation factors, *bam* and *bgcn*, have been associated with enhanced retention of GSCs in the niche of non-dysgenic germaria [62]. This model

is fully consistent with our observation that *bruno* suppression of ovarian atrophy is accompanied by a rescue of oogenesis at all stages, including enhanced maintenance of GSCs (Figure 6). It is additionally supported by the fact the *bruno* repression of *P*-element ovarian atrophy is independent of its mRNA target oskar, precluding *bruno*'s function in later stages of oogenesis from explaining its repressive effects (Figure 5).

Our observations with *bruno* reveal unexpected and novel role for developmental regulators of gametogenesis as determinants of germline tolerance of transposition. Interestingly, multiple regulators of female GSC maintenance and differentiation in *Drosophila melanogaster* exhibit recent or ongoing signatures of positive selection [63–65]. Tolerance to the selfish bacterial endosymbiont *Wolbacchia* has already been implicated in driving some of this adaptive evolution [66]. The fact that *bruno* alleles act as strong repressors of *P*-element hybrid dysgenesis suggests that another class of parasites, transposable elements, may also contribute to adaptive evolution of stem cell determinants.

MATERIALS and METHODS:

***Drosophila* Strains and Husbandry.** Recombinant inbred lines (RILs) from Population A were generously provided by Stuart Macdonald. Harwich (#4264), *Ced-12*^{c06760}*/CyO* (#17781), *Rab6*^{GE13031}*/CyO* (#26898), *Rab6*^{D23D}*/CyO* (#5821), and *ThrRS*^{K04203}*/CyO* (#10539), were obtained from the Bloomington *Drosophila* stock

center. Harwich was sib-mated for one generation to increase homozygosity. *Bruno* and *oskar* mutants and deficiencies, in single and double heterozygous combinations, were generously provided by Paul MacDonald. *Canton-S* was obtained from Richard Meisel. All flies were maintained in standard cornmeal media.

Phenotyping. Virgin RIL females were crossed to Harwich males, maintained at 25°C, and flipped onto fresh food every 3-5 days. Resulting F1 offspring were maintained at 25°C for 3 days or 21 days at which their ovaries were examined using a squash prep [56]. 21 day old females were transferred onto new food every 5 days as they aged to avoid bacterial growth. For the squash prep, individual females were squashed in a food-dye solution allowed to incubate for $\geq$ 5 minutes. After incubation, the slide was examined for the presence of stage 14, chorionated egg chambers, which preferentially absorb the dye. Females who produced $\geq$ 1 egg chambers were scored as having non-atrophied ovaries, and females producing 0 egg chambers were scored as having atrophied ovaries. A phenotyping schematic is provided in Figure 1A.

Crosses and phenotyping were performed for 656 RILs across 24 experimental blocks for 3 day-old F1 females, and 606 RILs across 21 experimental blocks for 21 day-old F1 females. If fewer than 21 F1 offspring were phenotyped for a given cross, it was discarded and repeated if possible. In total, we phenotyped >20 3-day old and 21 days-old F1 female offspring for 592 RILs and 492 RILs, respectively, and 660 RILs were assayed for at least one of the age groups.

QTL mapping. For age-class specific QTL mapping (3-day and 21-day old), the arcsine transformed proportion of F1 females with atrophied ovaries produced by each RIL was used as the response variable in a random effects multiple regression model that included experimental block and undergraduate experimenter.

$$\boldsymbol{asin}\sqrt{atrophy\ proportion} = Block\ + Experimenter$$

For the combined analysis of both age classes, we used the full set of arcsine transformed proportions, and accounted for female age as an additional fixed effect in the regression model.

$$\boldsymbol{asin}\sqrt{atrophy\ proportion} = Block\ + Experimenter + \ Age$$

All models were fit using the lmer function from the lme4 package[67].

The raw residuals of the regression models above were used as the phenotypic response for QTL analysis (Supplementary Tables 2-4), implemented with the DSPRqtl package[29] in R 3.02 [68]. The output yields a logarithm of the odds (LOD) score for the observed association between phenotype and genotype at 11,768 10 Kb intervals along the euchromatic arms of the X, 2 and 3rd chromosomes. The LOD significance threshold was determined from 1,000 permutations of the observed data, and the confidence interval around each LOD peak was identified by a difference of -2 from the LOD peak position (Δ2-LOD).

Broad sense heritability. Maternal genotype was added as a random effect to the models above, in order to determine the genetic variance in the phenotype (V^G). V^G was obtained by extracting the variance component for maternal genotype using the VarCorr() function from the nlme package [69]. Broad sense heritability (H^2) was then estimated proportion of overall variance (V^G/V^P).

Estimation of Founder Phenotypes and QTL phasing. To estimate the phenotypic effect of each founder at the QTL peak, we considered the residual phenotype for each used in QTL mapping and then determined the founder allele carried by the RIL at the LOD peak position [29]. RILs whose genotype at the LOD peak could not be assigned to a single founder with >95% probability were discarded.

Founder alleles were phased into phenotypic classes by identifying the minimal number of groups of alleles that describes phenotypic variation associated with the QTL peak [29]. Briefly, founder alleles were sorted based on their average estimated phenotypic effect, which was provided by the sampled RILs. Linear models containing all possible sequential partitions of founder alleles were then fit, and compared to a null model in which all founder alleles are in a single partition using an extra sum-of-squares *F*-test. The two-partition model with the highest *F*-statistic was retained and fixed only it if provided a significantly better fit ($P < 10^{-4}$) than the null model. The two partitions of founder haplotypes were then fixed, and all possible three-partition models were explored. This process was continued until the model fit could not be improved.

Identification of in-phase polymorphisms and TEs. Founders were assigned a "hard" genotype for all annotated TEs [70] and SNPs [29] in the QTL window if their genotype probability for a given allele was greater than 0.95 [29]. We then looked for alternate alleles that were in-phase with our inferred allelic classes [29,31]: the sensitive class (A3 and A5) and the tolerant class (A1, A2, A4, A6, and A7). A8 was excluded because its assignment to the sensitive or tolerant class differed between the data sets from 3-day old and 21-day old females.

Mutational analysis of candidate genes. Single and double heterozygote mutant virgin females (*mutant/balancer*) were crossed to Harwich males at 25°C. Because the vast majority of *Drosophila* lab stocks are *P*-element free, with the exception of any *P*-element derived transgenes, these crosses are dysgenic. Resulting F1 dysgenic female offspring were collected and aged at 25°C for 3-7 days, when their ovaries were assayed using the squash prep described above [56]. The incidence of ovarian atrophy was then compared between *mutant/+* and *balancer/+* siblings from the same cross.

Immunolabelling. Ovaries from 3-7 day old females offspring of dysgenic crosses were dissected and immediately fixed with 4% EM-grade methanol-free paraformaldehyde (Thermo Scientific). Ovaries were washed with 0.1% Triton X-100 in PBS, and blocked with 5% goat serum albumin (Sigma-Aldrich). Primary antibody concentrations were as follows: anti-Hts 1B1 1:4 (DSHB [71]), anti-Vasa

1:40 (DSHB), anti-Bruno 1:1000 (Provided by Paul MacDonald [46]), and anti-Orb 4H8 and 6H4 1:20 (DSHB [46]). Secondary antibody concentrations were 1:500.

Microscopy. Ovaries were visualized with a SP8 Upright Confocal DM6000 CFS (Leica) Microscope, outfitted with a 60X oil immersion lens. Images were collected using an EM-CCD camera (Hamamatsu) and LAS-AF software (Leica).

Acknowledgements. We are grateful to Stuart Macdonald, Paul MacDonald, and Richard Meisel for *Drosophila* strains, and Paul MacDonald for anti-Bruno antibodies. Ryan Castelluci, Ashka Shah and Wesley Adalume assisted in phenotyping atrophy among F1 offspring. Stuart Macdonald and Daniel Barbash provided helpful discussion and feedback on this manuscript. This research was funded by NSF DEB #1457800 to Erin Kelleher.

REFERENCES:

1. Chénais B, Caruso A, Hiard S, Casse N. The impact of transposable elements on eukaryotic genomes: from genome size increase to genetic adaptation to stressful environments. Gene. 2012;509: 7–15. doi:10.1016/j.gene.2012.07.042
2. Vitte C, Panaud O. LTR retrotransposons and flowering plant genome size: emergence of the increase/decrease model. Cytogenet Genome Res. Karger Publishers; 2005;110: 91–107. doi:10.1159/000084941

1 3. Sun C, Shepard DB, Chong RA, López Arriaza J, Hall K, Castoe TA, et al. LTR
2 retrotransposons contribute to genomic gigantism in plethodontid
3 salamanders. Genome Biol Evol. 2012;4: 168–83. doi:10.1093/gbe/evr139
4 4. Kunarso G, Chia N-Y, Jeyakani J, Hwang C, Lu X, Chan Y-S, et al. Transposable
5 elements have rewired the core regulatory network of human embryonic
6 stem cells. Nat Genet. 2010;42: 631–4. doi:10.1038/ng.600
7 5. Lynch VJ, Leclerc RD, May G, Wagner GP. Transposon-mediated rewiring of
8 gene regulatory networks contributed to the evolution of pregnancy in
9 mammals. Nat Genet. 2011;43: 1154–9. doi:10.1038/ng.917
10 6. Startek M, Szafranski P, Gambin T, Campbell IM, Hixson P, Shaw CA, et al.
11 Genome-wide analyses of LINE-LINE-mediated nonallelic homologous
12 recombination. Nucleic Acids Res. 2015; doi:10.1093/nar/gku1394
13 7. Rajaei N, Chiruvella KK, Lin F, Astrom SU. Domesticated transposase Kat1 and
14 its fossil imprints induce sexual differentiation in yeast. Proc Natl Acad Sci.
15 2014;111: 15491–15496. doi:10.1073/pnas.1406027111
16 8. Kapitonov V V, Jurka J. RAG1 Core and V(D)J Recombination Signal Sequences
17 Were Derived from Transib Transposons. Nemazee D, editor. PLoS Biol. Public
18 Library of Science; 2005;3: e181. doi:10.1371/journal.pbio.0030181
19 9. Silva-Sousa R, López-Panadès E, Casacuberta E. Drosophila telomeres: an
20 example of co-evolution with transposable elements. Genome Dyn. 2012;7:
21 46–67. doi:10.1159/000337127
22 10. Aminetzach YT, Macpherson JM, Petrov DA. Pesticide resistance via
23 transposition-mediated adaptive gene truncation in Drosophila. Science.

2005;309: 764–7. doi:10.1126/science.1112699

11. Mateo L, Ullastres A, González J. A Transposable Element Insertion Confers Xenobiotic Resistance in Drosophila. Feschotte C, editor. PLoS Genet. 2014;10: e1004560. doi:10.1371/journal.pgen.1004560

12. Hof AE van't, Campagne P, Rigden DJ, Yung CJ, Lingley J, Quail MA, et al. The industrial melanism mutation in British peppered moths is a transposable element. Nature. Nature Research; 2016;534: 102–105. doi:10.1038/nature17951

13. Dupuy AJ, Fritz S, Largaespada DA. Transposition and gene disruption in the male germline of the mouse. Genesis. 2001;30: 82–8. Available: http://www.ncbi.nlm.nih.gov/pubmed/11416868

14. Spradling AC, Stern D, Beaton A, Rhem EJ, Laverty T, Mozden N, et al. The Berkeley Drosophila Genome Project gene disruption project: Single P-element insertions mutating 25% of vital Drosophila genes. Genetics. 1999;153: 135–77. Available: http://www.pubmedcentral.nih.gov/articlerender.fcgi?artid=1460730&tool=pmcentrez&rendertype=abstract

15. Dorogova N V., Bolobolova EU, Zakharenko LP. Cellular aspects of gonadal atrophy in Drosophila P-M hybrid dysgenesis. Dev Biol. 2017;424: 105–112. doi:10.1016/j.ydbio.2017.02.020

16. Noutsopoulos D, Markopoulos G, Vartholomatos G, Kolettas E, Kolaitis N, Tzavaras T. VL30 retrotransposition signals activation of a caspase-independent and p53-dependent death pathway associated with

1 mitochondrial and lysosomal damage. Cell Res. 2010;20: 553–562.
2 doi:10.1038/cr.2010.48
3 17. Roy BA, Kirchner JW. Evolutionary dynamics of pathogen resistance and
4 tolerance. Evolution. 2000;54: 51–63. Available:
5 http://www.ncbi.nlm.nih.gov/pubmed/10937183
6 18. Mauricio R. Natural selection and the joint evolution of toleranceand
7 resistance as plant defenses. Evol Ecol. Kluwer Academic Publishers; 2000;14:
8 491–507. doi:10.1023/A:1010909829269
9 19. Blumenstiel JP. Evolutionary dynamics of transposable elements in a small
10 RNA world. Trends Genet. Elsevier Ltd; 2011;27: 23–31.
11 doi:10.1016/j.tig.2010.10.003
12 20. Yang P, Wang Y, Macfarlan TS. The Role of KRAB-ZFPs in Transposable
13 Element Repression and Mammalian Evolution. Trends Genet. 2017;
14 doi:10.1016/j.tig.2017.08.006
15 21. Senti K-A, Brennecke J. The piRNA pathway: a fly's perspective on the
16 guardian of the genome. Trends Genet. 2010;26: 499–509.
17 doi:10.1016/j.tig.2010.08.007
18 22. Aravin AA, Hannon GJ, Brennecke J. The Piwi-piRNA pathway provides an
19 adaptive defense in the transposon arms race. Science. 2007;318: 761–4.
20 doi:10.1126/science.1146484
21 23. Schaack S, Gilbert C, Feschotte C. Promiscuous DNA: Horizontal transfer of
22 transposable elements and why it matters for eukaryotic evolution. Trends
23 Ecol Evol. 2010;25: 537–546. doi:10.1016/j.tree.2010.06.001

24. Kelleher ES. Reexamining the P-Element Invasion of Drosophila melanogaster Through the Lens of piRNA Silencing. Genetics. 2016;203: 1513–31. doi:10.1534/genetics.115.184119

25. Kofler R, Hill T, Nolte V, Betancourt AJ, Schlötterer C. The recent invasion of natural Drosophila simulans populations by the P-element. Proc Natl Acad Sci. 2015;112: 201500758. doi:10.1073/pnas.1500758112

26. Hill T, Schlötterer C, Betancourt AJ. Hybrid Dysgenesis in Drosophila simulans Associated with a Rapid Invasion of the P-Element. PLoS Genet. 2016;12: e1005920. doi:10.1371/journal.pgen.1005920

27. Kidwell MG. Evolution of hybrid dysgenesis determinants in Drosophila melanogaster. Proc Natl Acad Sci U S A. 1983;80: 1655–9. Available: http://www.pubmedcentral.nih.gov/articlerender.fcgi?artid=393661&tool=pmcentrez&rendertype=abstract

28. Kidwell MG, Frydrk T, Novy J. The hybrid dysgenesis potential of Drosophila melanogaster from diverse temporal and geographic origins. Drosoph Inf Serv. 1983;59: 63–69.

29. King EG, Merkes CM, McNeil CL, Hoofer SR, Sen S, Broman KW, et al. Genetic dissection of a model complex trait using the Drosophila Synthetic Population Resource. Genome Res. 2012;22: 1558–66. doi:10.1101/gr.134031.111

30. King EG, Macdonald SJ, Long AD. Properties and power of the Drosophila Synthetic Population Resource for the routine dissection of complex traits. Genetics. 2012;191: 935–49. doi:10.1534/genetics.112.138537

31. Long AD, Macdonald SJ, King EG. Dissecting complex traits using the

1 Drosophila Synthetic Population Resource. Trends Genet. 2014;30: 488–495.
2 doi:10.1016/j.tig.2014.07.009
3 32. Bucheton A. I transposable elements and I-R hybrid dysgenesis in Drosophila.
4 Trends Genet. 1990;6: 16–21. Available:
5 http://www.ncbi.nlm.nih.gov/pubmed/2158161
6 33. Malone CD, Lehmann R, Teixeira FK. The cellular basis of hybrid dysgenesis
7 and Stellate regulation in Drosophila. Curr Opin Genet Dev. 2015;34: 88–94.
8 doi:10.1016/j.gde.2015.09.003
9 34. Schaefer RE, Kidwell MG, Fausto-Sterling A. Hybrid Dysgenesis in Drosophila
10 melanogaster: Morphological and Cytological Studies of Ovarian Dysgenesis.
11 Genetics. 1979;92: 1141–52. Available:
12 http://www.pubmedcentral.nih.gov/articlerender.fcgi?artid=1214061&tool=
13 pmcentrez&rendertype=abstract
14 35. Tasnim S, Kelleher ES. p53 is required for female germline stem cell
15 maintenance in P- element hybrid dysgenesis. Dev Biol. 2018;434: 215–220.
16 doi:10.1016/j.ydbio.2017.12.021
17 36. Kim-Ha J, Kerr K, Macdonald PM. Translational regulation of oskar mRNA by
18 bruno, an ovarian RNA-binding protein, is essential. Cell. 1995;81: 403–12.
19 Available: http://www.ncbi.nlm.nih.gov/pubmed/7736592
20 37. Wang Z, Lin H. Sex-lethal is a target of Bruno-mediated translational
21 repression in promoting the differentiation of stem cell progeny during
22 Drosophila oogenesis. Dev Biol. 2007;302: 160–168.
23 doi:10.1016/j.ydbio.2006.09.016

38. Jenny A, Hachet O, Závorszky P, Cyrklaff A, Weston MDJ, Johnston DS, et al. A translation-independent role of oskar RNA in early Drosophila oogenesis. Development. 2006;133. Available: http://dev.biologists.org/content/133/15/2827

39. Kanke M, Jambor H, Reich J, Marches B, Gstir R, Ryu YH, et al. oskar RNA plays multiple noncoding roles to support oogenesis and maintain integrity of the germline/soma distinction. RNA. 2015;21: 1096–109. doi:10.1261/rna.048298.114

40. Kidwell MG, Kidwell JF, Sved JA. Hybrid Dysgenesis in Drosophila melanogaster: A Syndrome of Aberrant Traits Including Mutation, Sterility and Male Recombination. Genetics. 1977;86: 813–33. Available: http://www.pubmedcentral.nih.gov/articlerender.fcgi?artid=1213713&tool=pmcentrez&rendertype=abstract

41. Engels WR, Preston CR. Hybrid dysgenesis in Drosophila melanogaster: the biology of female and male sterility. Genetics. 1979;92: 161–74. Available: http://www.pubmedcentral.nih.gov/articlerender.fcgi?artid=1213938&tool=pmcentrez&rendertype=abstract

42. Khurana JS, Wang J, Xu J, Koppetsch BS, Thomson TC, Nowosielska A, et al. Adaptation to P element transposon invasion in Drosophila melanogaster. Cell. 2011;147: 1551–63. doi:10.1016/j.cell.2011.11.042

43. Hartmann MA, Sekelsky J. The absence of crossovers on chromosome *4* in *Drosophila melanogaster* : Imperfection or interesting exception? Fly (Austin). Taylor & Francis; 2017;11: 253–259. doi:10.1080/19336934.2017.1321181

44. Brown JB, Boley N, Eisman R, May GE, Stoiber MH, Duff MO, et al. Diversity and dynamics of the Drosophila transcriptome. Nature. 2014;512: 393–399. doi:10.1038/nature12962

45. Schüpbach T, Wieschaus E. Female sterile mutations on the second chromosome of Drosophila melanogaster. II. Mutations blocking oogenesis or altering egg morphology. Genetics. 1991;129: 1119–36. Available: http://www.ncbi.nlm.nih.gov/pubmed/1783295

46. Filardo P, Ephrussi A. Bruno regulates gurken during Drosophila oogenesis. Mech Dev. 2003;120: 289–97. Available: http://www.ncbi.nlm.nih.gov/pubmed/12591598

47. Nilton A, Oshima K, Zare F, Byri S, Nannmark U, Nyberg KG, et al. Crooked, Coiled and Crimpled are three Ly6-like proteins required for proper localization of septate junction components. Development. 2010;137: 2427–2437. doi:10.1242/dev.052605

48. Casper J, Zweig AS, Villarreal C, Tyner C, Speir ML, Rosenbloom KR, et al. OUP accepted manuscript. Nucleic Acids Res. 2017;46: D762–D769. doi:10.1093/nar/gkx1020

49. Chakraborty M, VanKuren NW, Zhao R, Zhang X, Kalsow S, Emerson JJ. Hidden genetic variation shapes the structure of functional elements in Drosophila. Nat Genet. Nature Publishing Group; 2018;50: 20–25. doi:10.1038/s41588-017-0010-y

50. Thibault ST, Singer MA, Miyazaki WY, Milash B, Dompe NA, Singh CM, et al. A complementary transposon tool kit for Drosophila melanogaster using P and

1 piggyBac. Nat Genet. 2004;36: 283–287. doi:10.1038/ng1314
2 51. Parks AL, Cook KR, Belvin M, Dompe NA, Fawcett R, Huppert K, et al.
3 Systematic generation of high-resolution deletion coverage of the Drosophila
4 melanogaster genome. Nat Genet. 2004;36: 288–92. doi:10.1038/ng1312
5 52. Parisi MJ, Deng W, Wang Z, Lin H. The arrest gene is required for germline
6 cyst formation during Drosophila oogenesis. Genesis. 2001;29: 196–209.
7 Available: http://www.ncbi.nlm.nih.gov/pubmed/11309853
8 53. Kim-Ha J, Smith JL, Macdonald PM. oskar mRNA is localized to the posterior
9 pole of the Drosophila oocyte. Cell. 1991;66: 23–35. Available:
10 http://www.ncbi.nlm.nih.gov/pubmed/2070416
11 54. Xin T, Xuan T, Tan J, Li M, Zhao G, Li M. The Drosophila putative histone
12 acetyltransferase Enok maintains female germline stem cells through
13 regulating Bruno and the niche. Dev Biol. 2013;384: 1–12.
14 doi:10.1016/j.ydbio.2013.10.001
15 55. Bergman CM, Han S, Nelson MG, Bondarenko V, Kozeretska I. Genomic
16 analysis of *P* elements in natural populations of *Drosophila melanogaster*.
17 PeerJ. PeerJ Inc.; 2017;5: e3824. doi:10.7717/peerj.3824
18 56. Srivastav SP, Kelleher ES. Paternal Induction of Hybrid Dysgenesis in
19 *Drosophila melanogaster* Is Weakly Correlated with Both *P* -Element and *hobo*
20 Element Dosage. G3: Genes|Genomes|Genetics. 2017;
21 g3.117.040634. doi:10.1534/g3.117.040634
22 57. Ignatenko OM, Zakharenko LP, Dorogova N V, Fedorova SA. P elements and
23 the determinants of hybrid dysgenesis have different dynamics of

1 propagation in Drosophila melanogaster populations. Genetica. 2015;143:
2 751–9. doi:10.1007/s10709-015-9872-z
3 58. Ma X, Han Y, Song X, Do T, Yang Z, Ni J, et al. DNA damage-induced Lok/CHK2
4 activation compromises germline stem cell self-renewal and lineage
5 differentiation. Development. 2016;143: 4312–4323.
6 doi:10.1242/dev.141069
7 59. Li Y, Minor NT, Park JK, McKearin DM, Maines JZ. Bam and Bgcn antagonize
8 Nanos-dependent germ-line stem cell maintenance. Proc Natl Acad Sci.
9 2009;106: 9304–9309. doi:10.1073/pnas.0901452106
10 60. Ma X, Zhu X, Han Y, Story B, Do T, Song X, et al. Aubergine Controls Germline
11 Stem Cell Self-Renewal and Progeny Differentiation via Distinct Mechanisms.
12 Dev Cell. 2017;41: 157–169.e5. doi:10.1016/j.devcel.2017.03.023
13 61. Chen D, McKearin DM. A discrete transcriptional silencer in the bam gene
14 determines asymmetric division of the Drosophila germline stem cell.
15 Development. 2003;130: 1159–70. Available:
16 http://www.ncbi.nlm.nih.gov/pubmed/12571107
17 62. Jin Z, Kirilly D, Weng C, Kawase E, Song X, Smith S, et al. Differentiation-
18 Defective Stem Cells Outcompete Normal Stem Cells for Niche Occupancy in
19 the Drosophila Ovary. Cell Stem Cell. 2008;2: 39–49.
20 doi:10.1016/j.stem.2007.10.021
21 63. Civetta A, Rajakumar SA, Brouwers B, Bacik JP. Rapid evolution and gene-
22 specific patterns of selection for three genes of spermatogenesis in
23 Drosophila. Mol Biol Evol. 2006;23: 655–62. doi:10.1093/molbev/msj074

64. Bauer DuMont VL, Flores HA, Wright MH, Aquadro CF. Recurrent positive selection at bgcn, a key determinant of germ line differentiation, does not appear to be driven by simple coevolution with its partner protein bam. Mol Biol Evol. 2007;24: 182–91. doi:10.1093/molbev/msl141

65. Flores HA, DuMont VLB, Fatoo A, Hubbard D, Hijji M, Barbash DA, et al. Adaptive Evolution of Genes Involved in the Regulation of Germline Stem Cells in *Drosophila melanogaster* and *D. simulans*. G3: Genes|Genomes|Genetics. 2015;5: 583–592. doi:10.1534/g3.114.015875

66. Flores HA, Bubnell JE, Aquadro CF, Barbash DA. The Drosophila bag of marbles Gene Interacts Genetically with Wolbachia and Shows Female-Specific Effects of Divergence. Malik HS, editor. PLOS Genet. 2015;11: e1005453. doi:10.1371/journal.pgen.1005453

67. Bates D, Mächler M, Bolker B, Walker S. Fitting Linear Mixed-Effects Models Using lme4. J Stat Softw. 2015;67: 1–48. doi:10.18637/jss.v067.i01

68. R Development Core Team. R: A Language and Environment for Statistical Computing [Internet]. Vienna, Austria; 2008. Available: http://www.r-project.org

69. Pinheiro J, Bates D, DebRoy S, Sarkar D, R Core Team. {nlme}: Linear and Nonlinear Mixed Effects Models [Internet]. 2016. Available: http://cran.r-project.org/package=nlme

70. Cridland JM, Macdonald SJ, Long AD, Thornton KR. Abundance and distribution of transposable elements in two Drosophila QTL mapping resources. Mol Biol Evol. 2013;30: 2311–27. doi:10.1093/molbev/mst129

71. Zaccai M, Lipshitz HD. Role ofAdducin-like (hu-li tai shao) mRNA and protein localization in regulating cytoskeletal structure and function duringDrosophila oogenesis and early embryogenesis. Dev Genet. 1996;19: 249–257. doi:10.1002/(SICI)1520-6408(1996)19:3<249::AID-DVG8>3.0.CO;2-9

72. Hoskins RA, Carlson JW, Wan KH, Park S, Mendez I, Galle SE, et al. The Release 6 reference sequence of the Drosophila melanogaster genome. Genome Res. 2015;25: 445–58. doi:10.1101/gr.185579.114

Data Set	LOD Score	Peak Position	Δ2-LOD CI	% variation
3-days	19.59	2L:12260000	2L:12080000-12380000	14.2
21-days	17.22	2L:12250000	2L:12110000-12390000	14.8
combined	34.90	2L:12260000	2L:12120000-12350000	13.8

1

2 **Table 1. QTL peak positions.** The position of the major QTL peak for 3-day old F1
3 females, 21-day old F1 females, and the combined data set are shown. For each
4 analysis, the peak position an Δ2-LOD drop confidence interval in *Drosophila*
5 *melanogaster* genome release 6 (dm6 [72]) are provided. The percent of phenotypic
6 variation explained by the QTL peak is based on the genotype of each sampled RIL at
7 the LOD peak position.

8

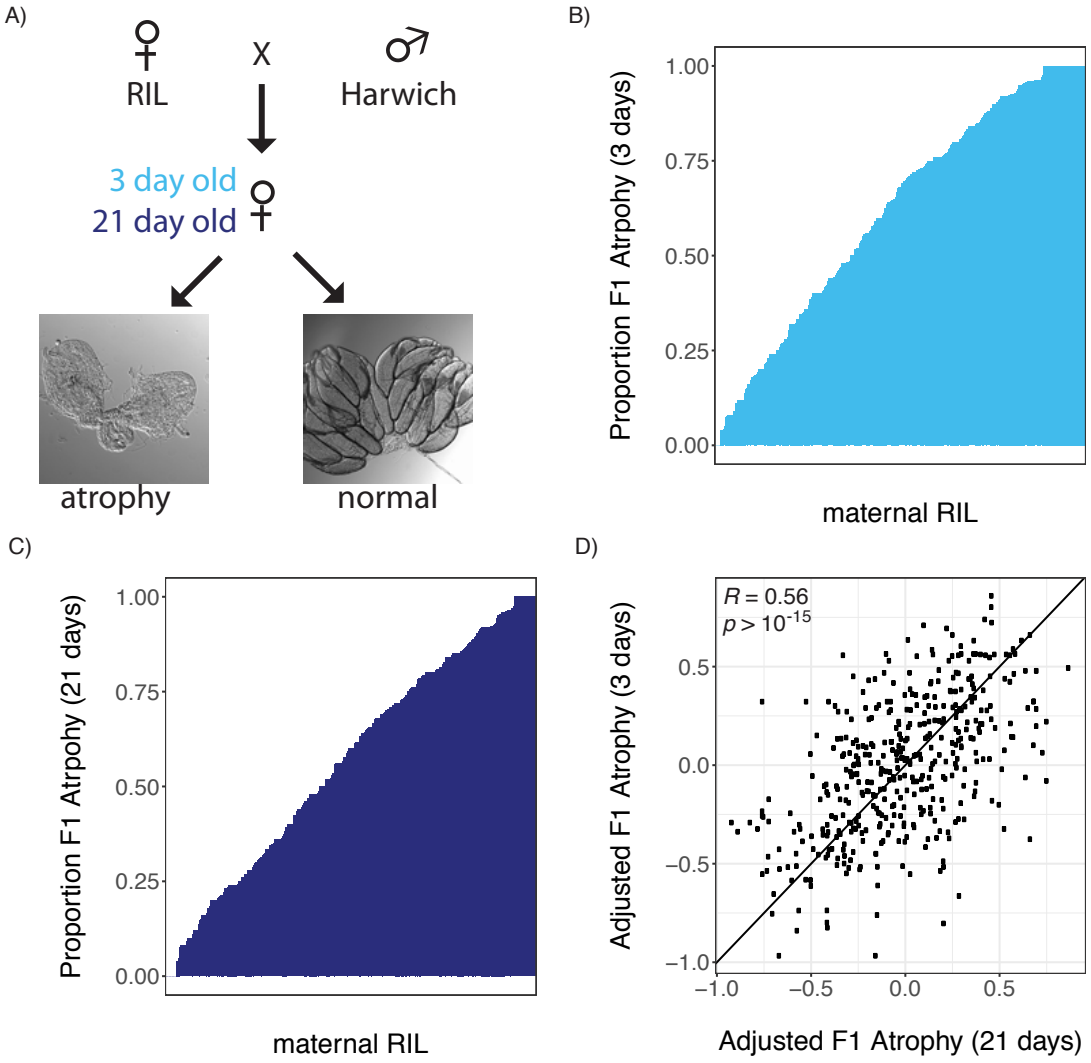

Figure 1. Heritable phenotypic variation in tolerance of *P*-element activity in the female germline. A) Crossing scheme for documenting variation in tolerance of *P*-element activity among RIL offspring. Representative images of atrophied and normal ovaries were published previously [35]. B and C) phenotypic variation in the proportion of 3-day old (B) and 21-day old (C) F1 female offspring of different RILs. RILs are sorted according the proportion of F1 atrophy observed in their offspring.

D) Scatterplot of the arsine-transformed proportion of F1 atrophy observed among 3-day old and 21-day old offspring of the same line, after accounting for the effects of experimenter and experimental block. Specifically, adjusted F1 atrophy values are the residuals of a random effects linear model including block and student experimenter (see methods).

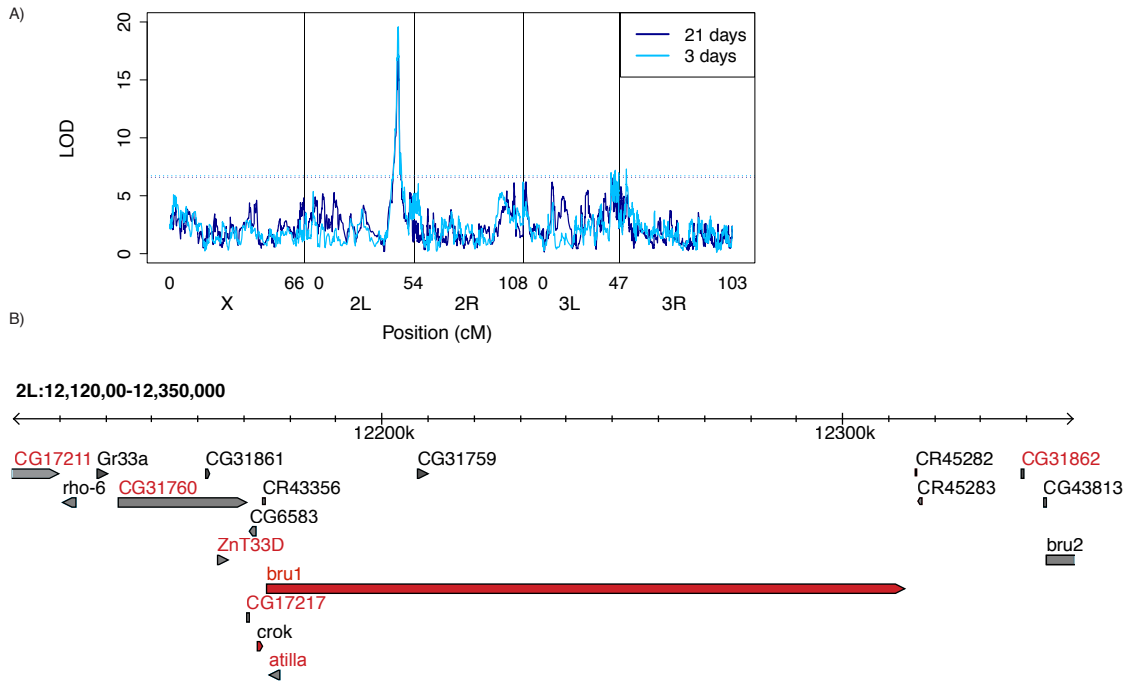

Figure 2. QTL mapping of variation in *P*-element tolerance. A) Logarithm of the odds ratio (LOD) of the observed association between maternal RIL genotype [29], and the adjusted proportion of F1 atrophy phenotype. Adjusted proportions of F1 atrophy are the residuals of a random effects linear regression that included experimenter and experimental block. Higher LOD scores correspond to stronger evidence of linkage, and significant LOD scores are above the threshold (dotted line), which was obtained from 1,000 permutations of the observed data. B) 2 LOD-drop confidence interval of the QTL peak based on a combined QTL analysis

1 including both 3-day old and 21-day old F1 females. Genes indicated by red letters

2 are potentially effected by polymorphisms in the RIL founders that are in phase the

3 inferred allelic classes (Figure 3 [48]). Gene boxes indicated red are highly

4 expressed in the *D. melanogaster* ovary [44].

A)

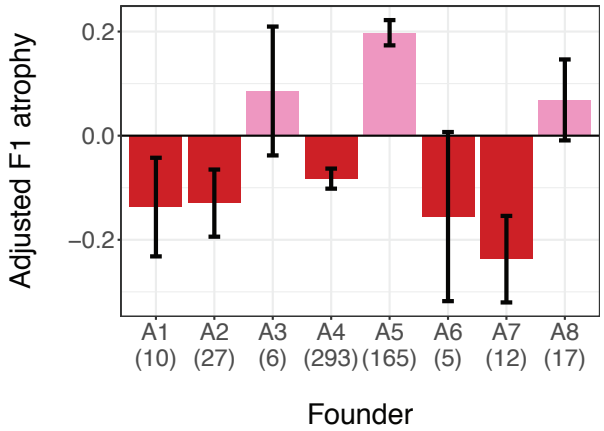

B)

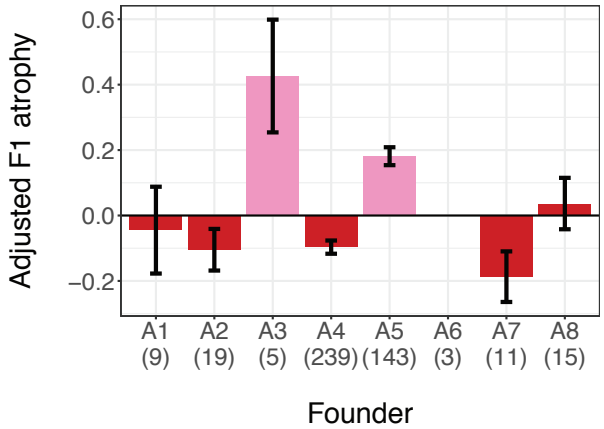

C)

A1 **TTCCACAAGGA**
A2 **TTCCACAAGGA**
A3 **TTCCAGAAGGA**
A4 **TTCCACAAGGA**
A5 **TTCCAGAAGGA**
A6 **TTCCACAAGGA**
A7 **TTCCACAAGGA**
A8 **TTCCACAAGGA**

5

Figure 3. Phenotypic classes of founder alleles at the major QTL peak. The adjusted F1 atrophy among 3-day old females A) and 21-day old females B) is shown for RILs carrying each of the 8 founder alleles. QTL phasing (see methods) detects two allelic classes for both the 3-day old and 21-day old phenotypes, a sensitive allele that increases the odds F1 ovarian atrophy (pink) and a tolerant allele that decreases the odds of F1 ovarian atrophy 1 (red). The assignment of founder alleles to phenotypic classes across ages is consistent for all founders except A8. C) An example in-phase SNP in the population A RIL founder genomes at 2L:12225285 (*Drosophila melanogaster* reference genome dm6 [72]).

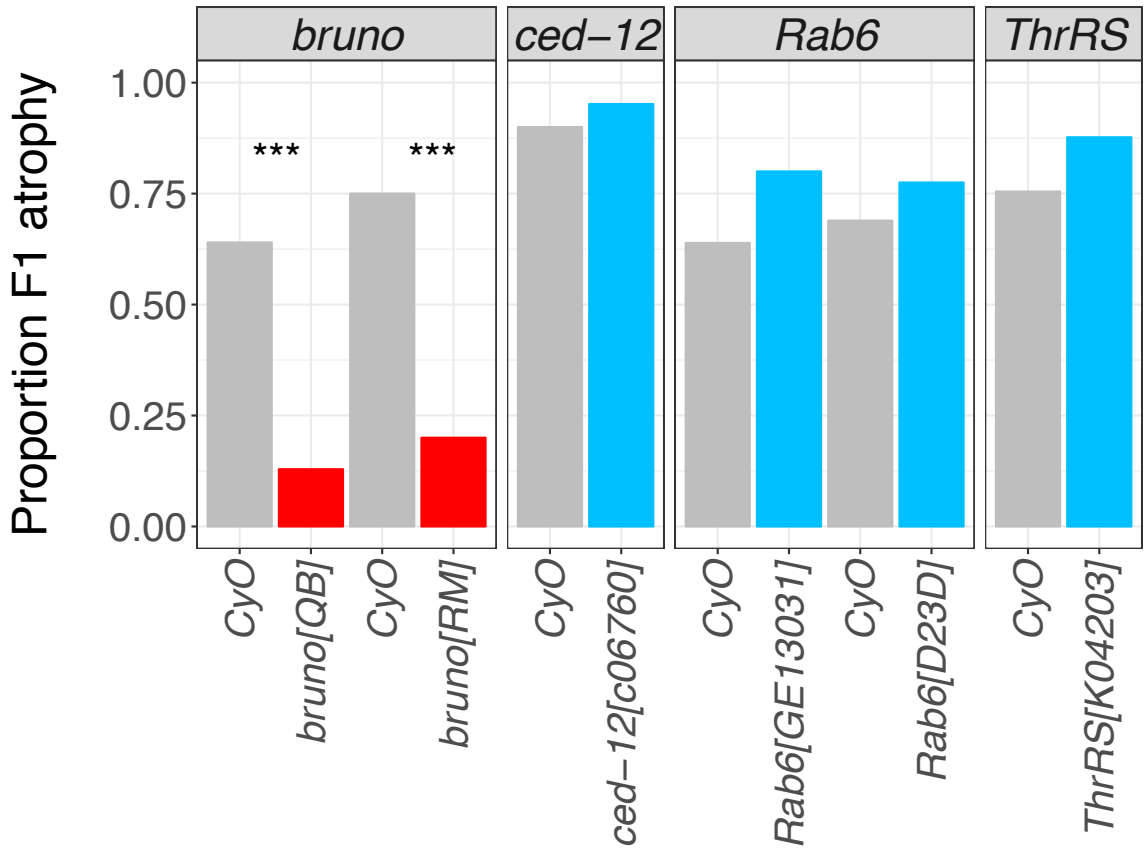

Figure 4. Mutational analysis of candidate genes. Loss of function heterozygotes for four candidate genes are compared to their siblings inheriting the balancer chromosome *CyO*, in order to detect zygotic effects on the incidence of ovarian atrophy among 3-7 day-old dysgenic F1 offspring. Only *bruno* alleles are significantly associated with altered odds of ovarian atrophy, acting as dominant suppressors of the atrophy phenotype.

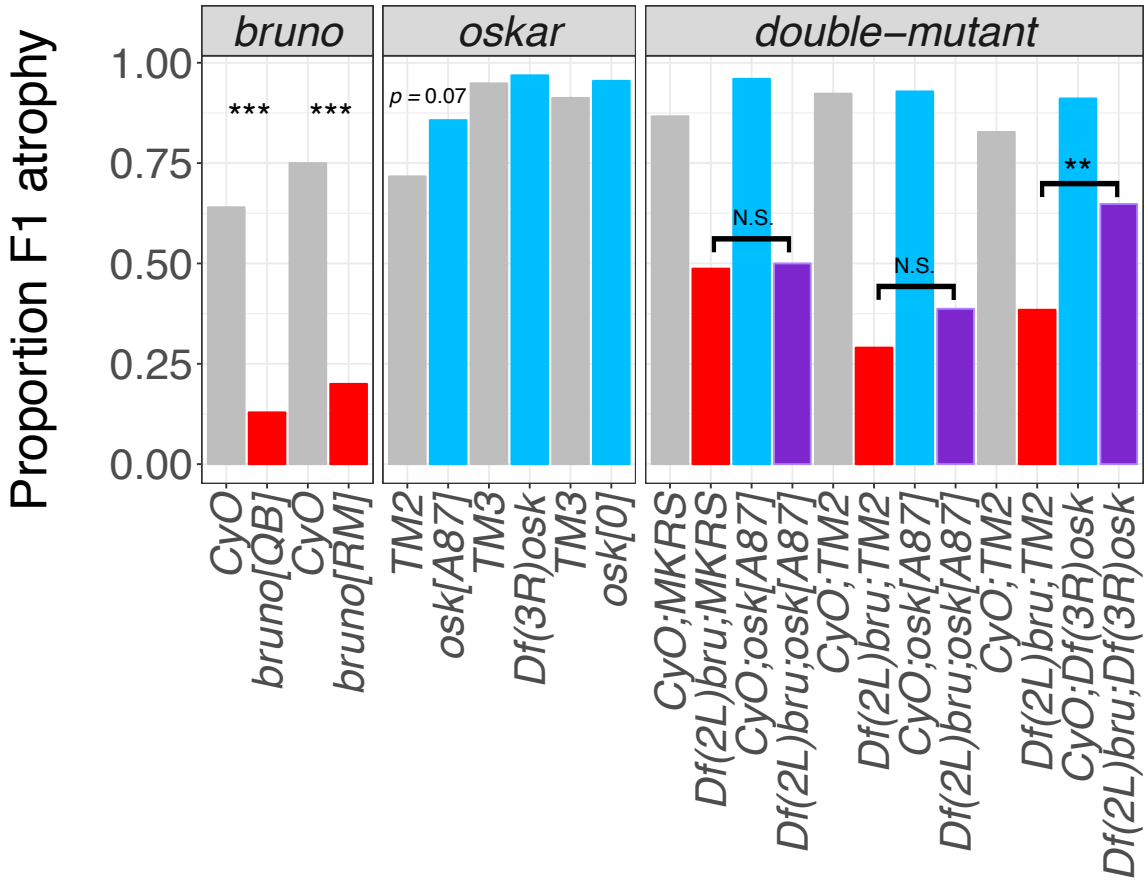

Figure 5. Mutational analysis of *bruno* and *oskar* single and double mutants. Single and double loss of function and deficiency heterozygotes for *bruno* and *oskar* are compared to their siblings inheriting the balancer chromosomes *CyO* (*bruno*) and *TM2*, *TM3* or *MKRS* (*oskar*), in order to detect zygotic effects on the incidence of atrophy among 3-7 day-old dysgenic F1 offspring. *Bruno* crosses are the same as in Figure 4, and are provided as a reference. While *bruno* alleles act as consistent dominant suppressors in both single and double mutants, *oskar* deficiencies and mRNA null mutants exhibit only stochastic effects on the atrophy phenotype,

1 suggesting that the mechanism of *bruno* suppression of F1 atrophy is independent

2 of *oskar* mRNA function.

3

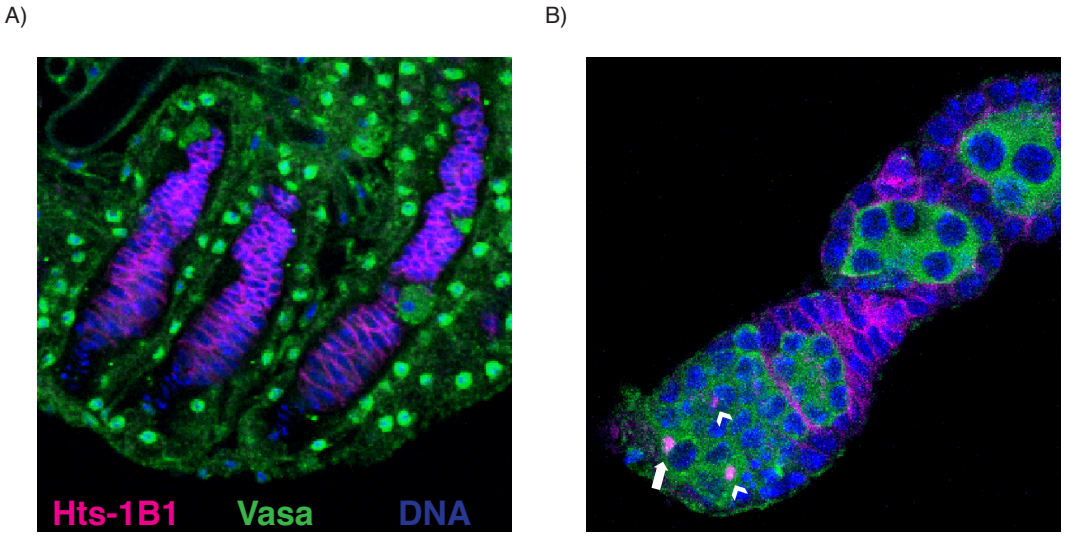

Figure 6. Reduced atrophy in *bruno^{QB}/+* ovaries is associated with enhanced retention of GSCs. A) Atrophied ovaries, which are less frequent in *bruno^{QB}/+* dysgenic females than their *CyO* siblings (Figure 4), lack any vasa-positive germline cells in the ovarioles, including GSCs. Nuclear Vasa external to Hts-1B1 corresponds to somatic ovarian sheath [35]. B) Non-atrophied (*i.e.* morphologically normal) ovaries, which are more common among *bruno^{QB}/+* dysgenic females than their *CyO* siblings (Figure 4), exhibit the full range of developing oocytes, including GSCs (white arrow). Arrowheads correspond to cystoblasts (CBs), the undifferentiated daughters of GSCs. Cytological markers are hu li tai shao (Hts-1B1), which labels somatic follicle cell membranes the circular fusomes of GSCs and CBs, and the spectrosomes that connect cells in the developing cyst, Vasa, which labels cytoplasm of germline cells and nuclei of the ovarian sheath, and DAPI staining of nuclear DNA.